

A high-resolution simulation of catastrophic rainfall over Uttarakhand, India

Prashant Kumar¹ · Bipasha P. Shukla¹ · Som Sharma² ·
C. M. Kishtawal¹ · P. K. Pal¹

Received: 6 June 2014 / Accepted: 10 October 2015 / Published online: 22 October 2015
© Springer Science+Business Media Dordrecht 2015

Abstract On 16 June 2013, intense and continuous rainfall together led to the collapse of moraine-dammed lake (Chorabari Lake) and devastated the entire land of Uttarakhand, Himalaya. This caused heavy floods in Uttarakhand (28°43′–31°27′ latitudes and 77°34′–81°02′ longitudes) along with unprecedented damage to life and property. Timely prediction and warning of such severe local weather systems over complex terrain are the first step towards disaster mitigation and bears huge societal impact. In this study, weather research and forecasting (WRF) model was configured at high spatial resolution (2 km) to simulate the Kedarnath heavy rainfall event over Uttarakhand region of India during 16–17 June 2013. Results showed that the WRF model was able to predict the Kedarnath heavy rainfall. Location and intensity of heavy rainfall were captured by the WRF model when verified with in situ measurements and satellite-retrieved rainfall products. Moreover, the explicit impact of topography in triggering this extreme weather event has been discussed using a diagnostic model which demonstrated that orographic component of rain rate is quite high over this region.

Keywords Heavy rainfall · High resolution · Numerical weather forecast · Forecast skill

1 Introduction

Rainfall is probably the most important parameter that is predicted by numerical weather prediction (NWP) models, though the skill of rainfall prediction is the poorest compared to other parameters, e.g., temperature and humidity (Kumar et al. 2014b). Since rainfall

✉ Prashant Kumar
kam3545@gmail.com; prashant22@sac.isro.gov.in

¹ Atmospheric Sciences Division, Atmospheric and Oceanic Sciences Group, Earth, Ocean, Atmosphere, Planetary Sciences and Applications Area, Space Applications Centre (ISRO), Ahmedabad 380015, India

² Space and Atmospheric Sciences Division, Physical Research Laboratory, Ahmedabad, India

affects society directly or indirectly, the accuracy and skill of rainfall prediction at varying spatio-temporal scales are strongly desirable. Rainfall forecast from the NWP models has improved over the last decades with the continuous progress in both numerical model and data assimilation techniques (Bauer et al. 2011; Benedetti et al. 2005; Kumar et al. 2014b; Lopez 2011). However, the prediction of extreme localized rainfall events over high complex terrain using NWP models remains a challenge due to insufficient model resolution, poor representation of orographic effects over complex terrain, lack of good-quality data over remote areas and insufficient land-surface parameterization.

In view of the paramount importance of the intense rainfall from economic, societal and scientific points, extensive work has been carried out over the years (Francis and Gadgil 2006; Guhathakurta and Rajeevan 2008; Khaladkar et al. 2009; SenRoy and Balling 2004; SinhaRay and De 2003). The analysis of 100 years of surface rainfall observations over the Indian monsoon region suggested that the mean monsoon seasonal rainfall has not changed significantly (Goswami et al. 2006), but several locations across India showed an increasing trend in heavy rainfall occurrence (>70 mm/day) during the summer monsoon season. Moreover, increase in extreme rainfall (>120 mm/day) events during the Indian monsoon has been particularly strong in the last 50 years (Goswami et al. 2006). Kishtawal et al. (2010) assessed the impact of urbanization on the heavy rainfall climatology during the Indian summer monsoon. Rajeevan et al. (2008) analysed the variability and trends of extreme rainfall events over India with the help of years of gridded daily rainfall data. Guhathakurta et al. (2011) found that the extreme rainfall and flood risk are increasing significantly in the country except some parts of central India.

Various sensitivity experiments (Bohra et al. 2006; Das et al. 2006; Kumar et al. 2008) were performed to assess the impact of NWP model for extreme rainfall events. Das et al. (2006) used the MM5 mesoscale model to predict a cloudburst event over the Himalaya and demonstrated that the MM5 model was able to predict the heavy rainfall event. However, the location of the cloudburst was displaced by tens of kilometres. Kumar et al. (2008) performed a number of experiments with the WRF model and suggested that the highly localized, heavy rain was the result of an interaction of synoptic-scale weather systems with the mesoscale, coastal land-surface features. Moreover, WRF system was able to reproduce the heavy rainfall event and the associated dynamical and thermodynamical features. Bohra et al. (2006) suggested that the implementation of very high resolution global/regional models with advanced data assimilation techniques could significantly enhance the usefulness of the NWP model. Chang et al. (2009) assessed the impact of land-surface parameterizations on the simulation of the Mumbai heavy rain event. They performed sixteen numerical experiments for various land-surface schemes with different land-use/land-cover conditions and showed that the rainfall prediction from the WRF model was better than the MM5 model in terms of both location and intensity. Anabor et al. (2009) studied mesoscale convective system (MCS) events over south-eastern part of the South America using the WRF model at 10-km spatial resolution. Wang et al. (2014) studied the rainstorm process occurred in the North China using the WRF model and focused on net budget of water vapour. Authors found that net budget of water vapour was always positive during the rainstorm process because the zonal deficit was much smaller than the meridional surplus. Wang et al. (2014) used one-way interactive nested domain having spatial resolution of 27, 9 and 3 km. Srinivasan (2013) provided prospective views on ways to predict, manage and adapt to heavy rainfall events in the future. However, prediction of high-impact rain events over complex topography through numerical models still remains a field of ongoing research.

Considering these aspects in the present study, the WRF model was configured at high resolution to predict an extreme rainfall event over Western Himalayan region on 16–17 June 2013, which devastated the state of Uttarakhand, India. The scope of this study is to assess the skill of the WRF model at high spatial resolution (2 km) over complex terrain to simulate the catastrophic rainfall and understand the nature of the anomalous behaviour of this event, and to suggest how future disasters in this part of the world might be better anticipated and predicted through the use of high-resolution regional models. Moreover, the linkage of topography in triggering this high-impact event has also been discussed using a diagnostic model.

2 Uttarakhand disaster

The upper Himalayan territories of Himachal Pradesh and Uttarakhand are mainly covered with forests and mountains. These areas, besides being important pilgrimage centres, are also famous as tourist attractions especially during the hot summer months of the Indian subcontinent. However, this region is prone to various forms of geological and meteorological hazards. In addition, there is a clear indication that not only the frequency of such hazards is increasing with time but also their intensity and impact on the lives and livelihood of inhabitants of the region is increasing in severity.

In year 2013, the monsoon winds arrived early in India and reached this region almost 2 weeks in advance (India Meteorological Department (IMD) Report 2013). The glaciers melt faster when water falls on ice, and the massive run-off began to engorge catchment that caused heavier flow in the rivers. During 14 to 17 June 2013, Uttarakhand received continuous heavy rainfall, and when this was combined with the melting snow (due to high temperature during summer season) resulted in the formation and expansion of moraine-dammed lakes, creating a potential danger from dammed lake outburst floods. On 16 and 17 June 2013, heavy rains together with moraine-dammed lake (Chorabari Lake) burst caused flooding of Saraswati and Mandakini Rivers in Rudraprayag district of Uttarakhand (Dobhal et al. 2013). This had caused severe floods, landslides, large-scale loss of lives, properties and damages. Prolonged heavy down pour on 16 and 17 June 2013 resembled ‘cloud burst’-type event (except for amount of precipitation of 100 mm/h) in the Kedarnath valley and surrounding areas that damaged the banks of River Mandakini for 18 km between Kedarnath and Sonprayag, and completely washed away Gaurikund (1990 m asl), Rambara (2740 m asl) and Kedarnath (3546 m asl) towns (Dobhal et al. 2013). The roads and footpath between Gaurikund and Kedarnath were also damaged. There were reports of loss of large number of human lives and damage to the property and livestock. On 17 June alone, the state of Uttarakhand received more than 340 mm of rainfall, which was 375 % more than the daily normal (65.9 mm; Dube et al. 2013; India Meteorological Department (IMD) Report 2013). The development of this convective activity over Indian region is illustrated in Fig. 1 using visible channel images from Kalpana satellite. It can be clearly seen that westerlies advect the optically thick clouds over the north-western Himalayan region where they remained stationary during 16–17 June and caused large-scale destruction.

3 Model description

The mesoscale model employed in this study was the weather research and forecasting (WRF; Skamarock et al. 2008) model version 3.4. The WRF is a limited area, non-hydrostatic, primitive equation model with multiple options for various physical

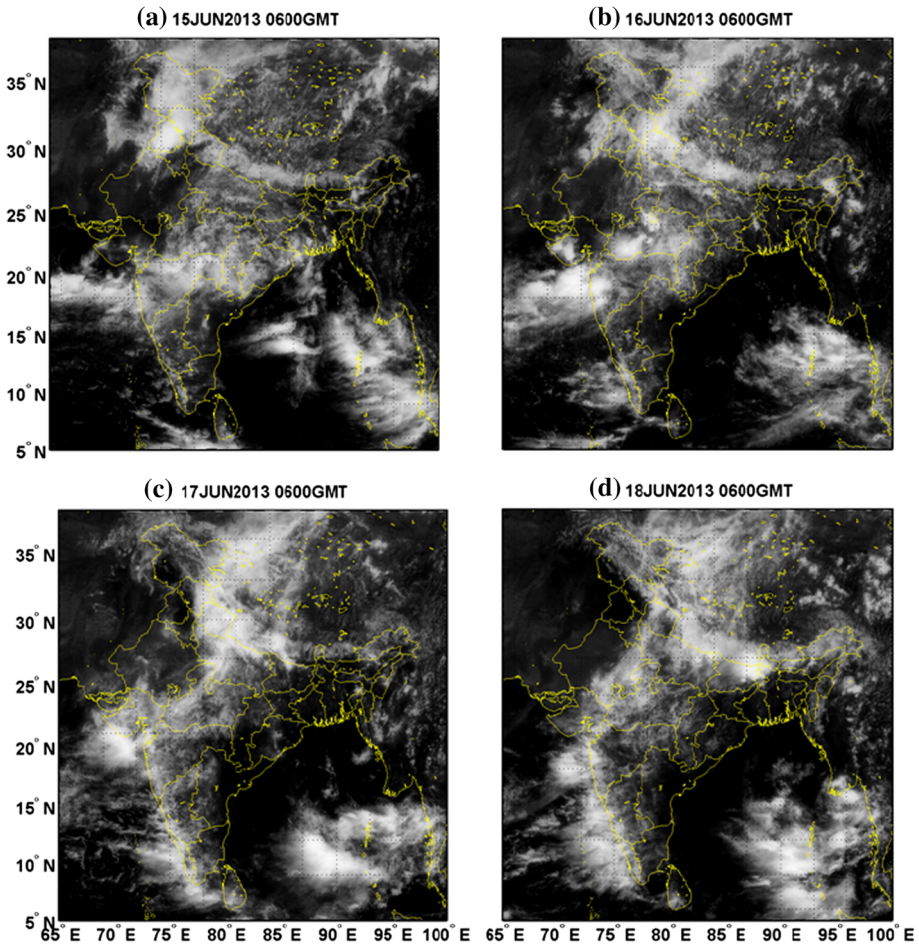


Fig. 1 Evolution of large-scale convective system over northern India during 15–18 June 2013 using Kalpana AVHRR visible channel

parameterization schemes. This version employed Arakawa C-grid staggering for the horizontal grid and a fully compressible system of equations. The time-split integration used a third-order Runge–Kutta scheme with a smaller time step for acoustic and gravity wave modes. A more complex micro-physics scheme WSM6 used here is an extension of the single-moment 3-class (WSM3) scheme, which additionally predicts the mixing ratio of snow and graupel hydrometeors. Hong and Lim (2006) found that for high-resolution grid, the amount of rainfall increases and peak intensity is stronger as the number of hydrometers increases. The cumulus physics scheme was Kain–Fritsch (KF) (Kain and Fritsch 1990) for the cumulus convection parameterization scheme for outer domain only, and the Yonsei University (YSU) scheme for planetary boundary layer (Hong and Dudhia 2003; Hong and Pan 1996). The KF scheme is a mass-flux parameterization scheme that determines the strength of convection from convective available potential energy when deep convection is triggered (Kain and Fritsch 1990). The KF scheme mixes the air by convection as well as related updrafts and downdrafts, and it rigorously conserves mass,

thermal energy, total moisture and momentum (Kain and Fritsch 1993). The YSU planetary boundary layer (PBL) is responsible for vertical sub-grid-scale fluxes due to eddy transports in the whole atmospheric column, not just the boundary layer (Hu et al. 2010). Thus, when a PBL scheme is activated, explicit vertical diffusion is de-activated with the assumption that the PBL scheme will handle this process. The PBL schemes determine the flux profiles within the well-mixed boundary layer and the stable layer and thus provide atmospheric tendencies of temperature, moisture (including clouds) and horizontal momentum in the entire atmospheric column. The Rapid Radiative Transfer Model (RRTM; Mlawer et al. 1997) and Dudhia scheme (Dudhia 1989) were used for long-wave and short-wave radiation, respectively. These physics parameterization schemes have been shown to be useful when simulating WRF precipitation events over Indian region in earlier studies (Kumar et al. 2014b; Wang et al. 2014). WRF forecast experiment was conducted with a two-way nested domain, i.e., outer domain (domain 1: longitude 72.6°E–85.4°E and latitude 25.3°N–36.3°N) consisting of 240×240 grid points with 6-km horizontal grid resolution and inner domain (domain 2: longitude 75.3°E–81.7°E and latitude 27.7°N–33.3°N) consisting of 361×361 grid points with 2-km horizontal grid resolution. Wang et al. (2014) used one-way nesting to run the WRF model at high (3-km) spatial resolution for net budget of water vapour in North China, whereas, in this study, two-way nesting was used to perform the model simulations, where domains at different grid resolutions were run simultaneously and communicate with each other. The coarser domain provided boundary value for the nest, and the nest fed its calculation back to the coarser domain. The high-spatial-resolution (2-km) domain resolved the complex topography more accurately, and the two-way nesting communicates this information from finer resolution domain to coarser resolution domain which improves the simulations of coarser domain and subsequently improves the model prediction. Topography, land use/land cover and other geographical informations at 30-s resolution were taken from United States Geological Survey (USGS). The model had 36 vertical levels with top of the model atmosphere located at 10 hPa. WRF model simulation starts from 0000 UTC 16 June 2013 for 24-h prediction valid at 0000 UTC 17 June 2013. NCEP GDAS analyses available at $1^\circ \times 1^\circ$ spatial resolution are used to produce initial and lateral boundary conditions for WRF model run.

4 Influence of orographic and synoptic conditions preceding the catastrophic rainfall

4.1 Orographic effects

The orographic precipitation is enhanced in the range of 200–300 % over the complex Himalaya terrain (Barros et al. 2000, 2004). In this case, not only the elevation but also the spatial arrangement of the topographic gradients determines the precipitation patterns. The elevation map of study domain is shown in Fig. 2 which represents very complex terrain over this region. The enhancement of precipitation as it interacts with the underlying topography is probably one of the major causes of high-impact rain events over this region (Das et al. 2006). To further investigate the role of topography, a diagnostic model VDEL based on topographically induced vertical motion (Sinclair 1994) is used to estimate orographic precipitation for the catastrophic rainfall event. This model is based on the premise that the enhancement of orographic precipitation is due to forced uplift of moist air over elevated terrain. As such, the vertical velocity near the ground (w_s) is considered as a

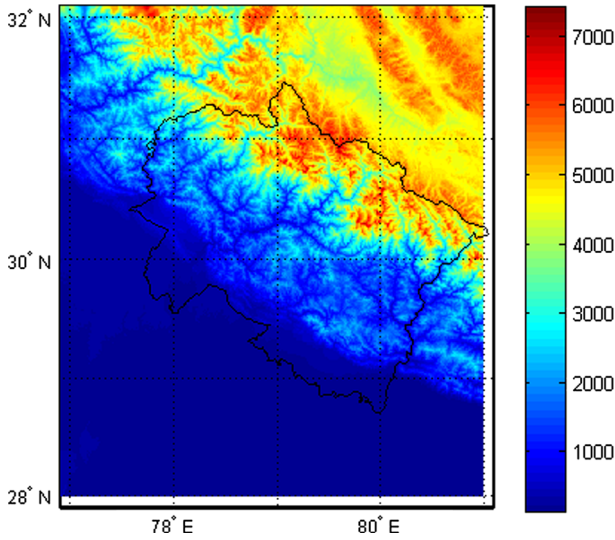


Fig. 2 Elevation map of the state of Uttarakhand (m)

function of low-level flow (V_s) and topography of height $z_s(x, y)$ (hence the name VDEL, Thompson et al. 1997) and is approximated by:

$$w_s \approx -\rho_s g V_s \cdot \nabla z_s$$

where ρ_s is the relative density of air at the surface and g is the acceleration due to gravity.

In VDEL model, condensation arises by means of saturated adiabatic ascent. The amount of condensate produced at pressure level p , per unit time is proportional to the rate of ascent, $w(p)$, which is parameterized as function of height. The vertical velocity profile is composed in two parts: the large-scale w_m from the model and terrain-induced w_t such that

$$w(p) = w_m(p) + w_t(p)$$

and

$$w_t(p) = w_s G(p)$$

where $G(p)$ is the function that specifies how the terrain-induced vertical velocity decreases from the surface to zero at the top of the condensing layer. The exact form of $G(p)$ can be found in Sinclair (1994). It is to be noted here that the large-scale vertical motions caused by fronts and other processes in the free atmosphere also contribute to ascent over mountains. But the focus of the present study is to diagnose the contribution of topography in triggering the heavy rainfall event. Finally, the rainfall rate at the ground is obtained as

$$R = \frac{\lambda_S}{g} \int_0^{p_{del}} \delta F \lambda(p) \cdot w(p) dp$$

where λ is a factor dependent on relative humidity (RH) and is responsible for modulating rainfall with moisture availability. It is well known that orographic rainfall is a strong function of low-level RH . The form of λ as given in Sinclair (1994) reflects this

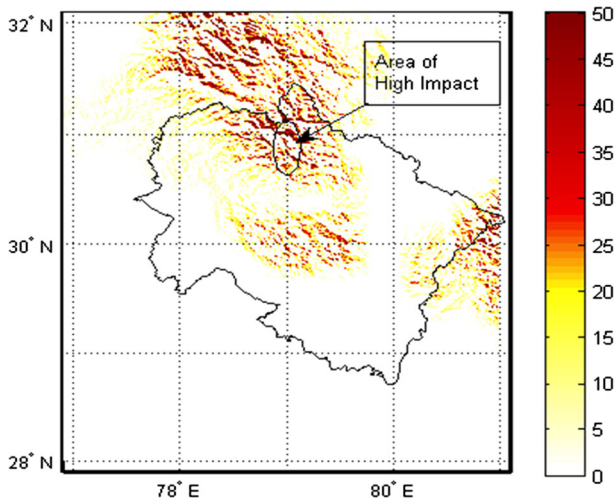


Fig. 3 Orographic precipitation rate (mm/h) as simulated by VDEL model

dependence as well as the modulation of mid-tropospheric condensation by ambient RH . The form of δF is discussed in detail by Sinclair (1994), and it mainly models the condensation rate at each pressure level. When we calculate the condensate at each height, the variable fall times of hydrometeors can be included at each vertical layer. This is done by assuming that the condensate drifts a vector distance $V\Delta t$ downwind before landing, where Δt is the sum of the formation plus the fall time to the surface from the vertical layer.

The VDEL model can be implemented for a single sounding measurement as well as for a numerical model. In the present case, VDEL model is initialized from WRF model on 16 June 2013 and the orographic precipitation obtained from the VDEL model is shown in Fig. 3. It can be clearly observed from Fig. 3 that the orographic component of rain rate is quite high inside the marked ellipse which was the area of maximum impact. This simulation suggests that the topography, in particular with its orientation to the low-level wind fields, and the moisture availability had a major role in this extreme precipitation event.

4.2 Synoptic condition

The mean sea-level pressure and low-level (850 hPa) winds available from ECMWF analysis at 0000 UTC during 13 June 2013 to 16 June 2013 are shown in Fig. 4, which shows the location of monsoon low changed from day to day during this period. A monsoon low-pressure area occurred over the north-west Bay of Bengal on 13 June 2013 (Fig. 4a) which had a general north-westward movement. The ECMWF analysis of the lower tropospheric wind and sea-level pressure fields showed the progress of south-east monsoon current from south- to north-west up to Uttarakhand and simultaneously movement of a western disturbance across north India from west to east. The westerlies and the monsoon system virtually locked over the Uttarakhand and neighbouring regions during this period (Fig. 4d). The strength of the monsoon wind flow was relatively weaker in the Himalayan region (Fig. 4d), but as a result of this system, a strong south-easterly wind flow over Uttar Pradesh, Uttarakhand and Himachal Pradesh pumped moisture into the region from both the Arabian Sea and Bay of Bengal. The analysis suggested that due to strong

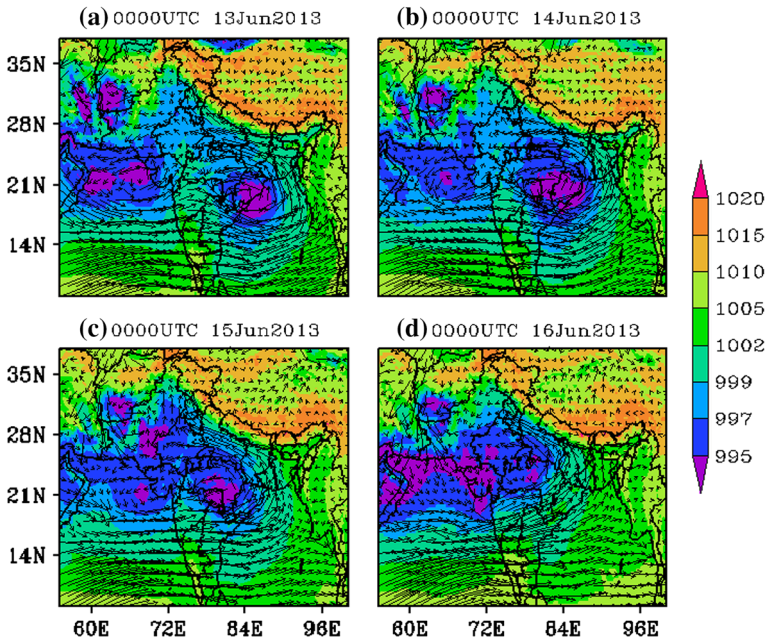


Fig. 4 Spatial distribution of mean sea-level pressure (*shaded*; hPa) and low-level (850 hPa) winds (vector; m/s) from ECMWF analysis at 0000 UTC of **a** 13 June, **b** 14 June, **c** 15 June and **d** 16 June 2013

interaction between an oncoming trough in the westerlies and the strong south-easterly monsoon wind flow in association with a monsoon low-pressure system over the north Indian region, resulting development of lower tropospheric wind convergence over the Uttarakhand and neighbouring regions (IMD report 2013). This, coupled with strong orographic effect due to high terrain when coupled by the strong moisture feeding from both the Arabian Sea and Bay of Bengal, triggered heavy rainfall activity downstream of the trough, over the north Indian region in a similar moisture pumping phenomena as observed during the Leh flash flooding storm of 2010 (Rasmussen and Houze 2012). However, the Uttarakhand episode was unique in that the line of convergence of the two weather systems was nearly stationary for hours at a time, due to orographic focussing of convective cell activity over limited region (Buzzi and Foschini 2000) resulting in huge amount of accumulated rainfall over the north-western Himalayan region causing widespread flooding.

5 Results and discussions

Three different merged rainfall products available from CMORPH, JAXA GSMaP and TRMM 3B42 (Kumar et al. 2014b) at spatial resolution of 8, 10 and 25 km, respectively, were used in this study to assess the skill of the WRF model rainfall prediction (Fig. 5). All the three merged rainfall products (Fig. 5a–c) represented the heavy rainfall over the Uttarakhand region. More intense rainfall was produced by CMORPH product locally over Uttarakhand compared to TRMM and JAXA rainfall products. JAXA and TRMM rainfall products showed larger spatial distribution compared to CMORPH rainfall product; 24-h

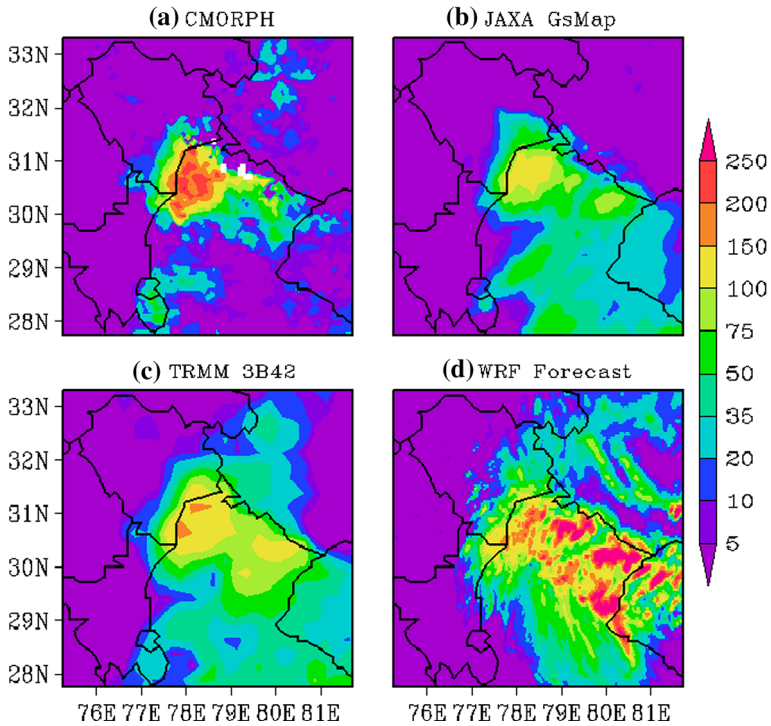


Fig. 5 Spatial distribution of accumulated merged rainfall (mm) product from **a** CMORPH, **b** JAXA GsMap and **c** TRMM 3B42 product during 0000 UTC 16 June 2013–0000 UTC 17 June 2013. **d** Spatial distribution of 24-h rainfall forecast (mm) from WRF model

accumulated rainfall forecast from WRF model (at 2-km spatial resolution) was able to reproduce the maximum rainfall over the Uttarakhand region, and the spatial distribution of rainfall was similar to TRMM- and JAXA-derived rainfall data. WRF model predicted rainfall was higher in intensity compared to TRMM and JAXA rainfall products. Over the Himalayan high orographic region, JAXA rainfall showed very small values which was higher in TRMM rainfall product. The possible reason may be that rain-gauge informations are used in the TRMM 3B42 rainfall product which shows more realistic representation of rainfall over this region. Satellite estimated merged rainfall product shown the light rainfall over the south-eastern part of the Punjab which missed in the WRF rainfall forecast. Moreover, WRF model overestimated the rainfall over the Himalayan’s high topographic region. Two ground stations, Nainital, Uttarakhand (longitude 79.46°E and latitude 29.36°N), and Champawat, Uttarakhand (longitude 80.09°E and latitude 29.34°N), measured rainfall are used in this study to compare the WRF model predicted hourly rainfall. Figure 6 shows that WRF model predicted rainfall is able to capture the observed rainfall over Nainital region, except large mismatches in initial forecast hours. These discrepancies may be due to initial model spin-up period. WRF model is slightly under-predicted the rainfall beyond 19-h forecasts for Nainital station. Large overestimation was found in WRF model simulated rainfall over the Champawat region, though the trend was similar.

Figure 7 shows the integrated value of hydrometer (snow, ice, graupel and rain) forecast at the time (1500 UTC 16 June 2013) of intense rainfall (reported by Indian Meteorological

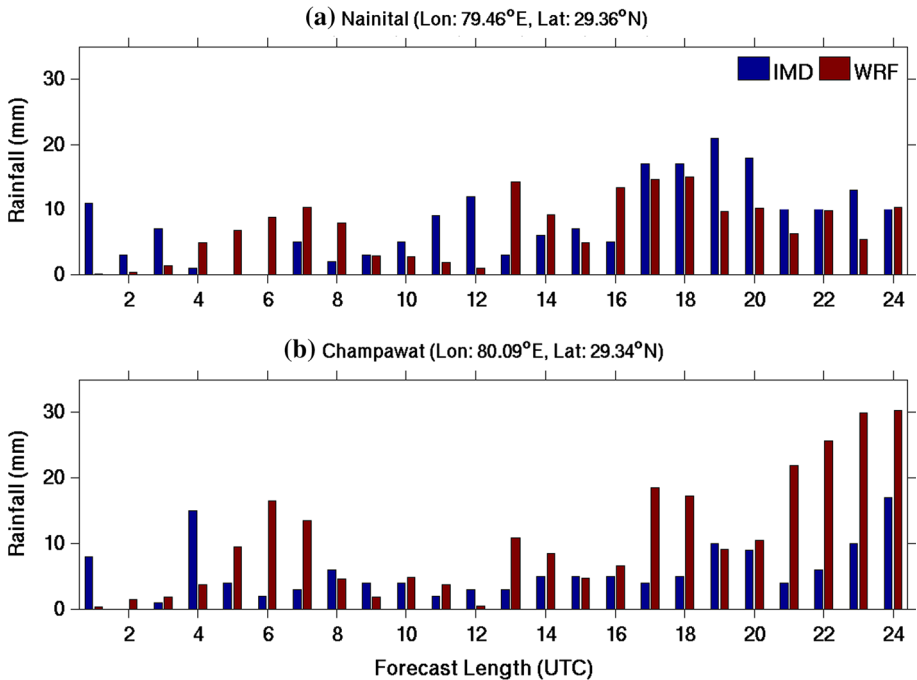


Fig. 6 Comparison of the WRF model hourly rainfall forecast with ground observations over Nainital and Champawat, Uttarakhand, regions

Department, India). Storm-producing clouds generally contain a deep mixed-phase zone and also form the precipitation in the ice phase as hail, graupel and snow particles. In this case, WRF model is able to simulate the hydrometeor at the time of heavy rainfall. It was evident from Fig. 7 that high value of snow and graupel occurred just over the Kedarnath region. At the same time, rainfall forecast within 1 h (Fig. 7d; 1500 UTC to 1600 UTC) also showed that WRF model was able to capture this heavy rainfall. It was interesting to note here that WRF model was able to predict the heavy rainfall over the Kedarnath region where integrated values of all the hydrometers were large compared to other locations.

According to Doswell et al. (1996), certain ingredients needed to be in place for a high precipitation event, which included low tropospheric moisture inflow, lifting mechanism for transporting the moisture to higher level and instability to support vertical motion. Simultaneously other factors acting synergistically: non-precipitating environment in the neighbourhood to ensure that the moisture is not lost in the way, concentration of moisture coupled with upper-tropospheric divergence over a small region escalate severe localized precipitation (Reale et al. 2001). To study the dynamics at the time of the event, we investigated vertical development of different atmospheric variables in a north–south cross section. As explained earlier, the large-scale transport of moisture triggering the event was carried through a southerly low-level jet, so it was natural to consider the south-to-north variation of the meteorological parameters.

As seen from Fig. 8a, the relative humidity was uniformly high at lower troposphere (surface to 500 hPa) and dry in upper levels that provided the required source of moisture, inhibiting the entrainment of dry air into the updrafts. It was interesting to note from

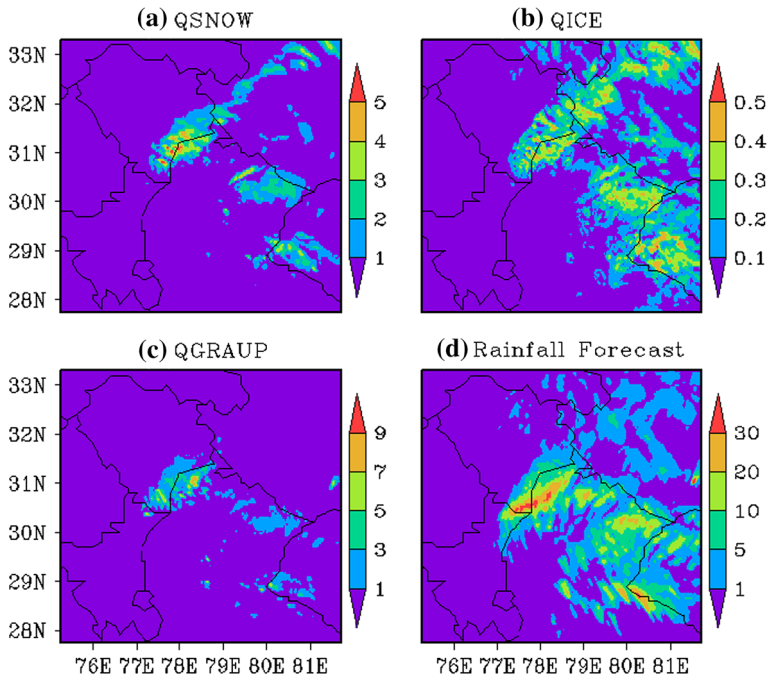


Fig. 7 Spatial distribution of integrated value of hydrometer **a** qsnow (kg/kg), **b** qice (kg/kg) and **c** qgraupel (kg/kg) at the time of heavy rainfall (1500 UTC 16 June 2013). **d** Spatial distribution of rainfall forecast (mm) from WRF model between 1500 UTC and 1600 UTC 16 June 2013

Fig. 8b that the model simulated a strong and isolated region of lower-level moisture convergence just south of 31 N (centre of the extreme event) with upper-level divergence denoted by negative values of moisture convergence. Additionally, zonal and meridional components of the vertically integrated atmospheric moisture transport fields were calculated at the time of event (Fig. 9). Total moisture content of the atmosphere plays a vital role in the development of hazardous atmospheric phenomena such as thunderstorms and severe weathers (Howarth 1983). The spatial map of vertically integrated moisture transport (in vector; Fig. 9) characterized by dense vectors in the region of interest which signified ample supply of moisture to maintain saturated upslope motion resulting in quasi-stationary system.

Figure 10a illustrates the model simulated vertical wind profile, showing very strong updrafts, which is typical of orographic forcing triggering instability. The slight tilt of the updrafts (in this case, southwards) was a common feature associated a severe convection that extended the life of the storm, because the precipitation does not fall directly into the updraft and the warm air intake can continue (Ludlam 1963). Similarly Fig. 10b demonstrates the south–north cross section of the horizontal divergence profile, in which divergence maxima was seen at the location of the event, with upper-level maxima tilted towards south, which was consistent with the precipitation pattern.

In Fig. 11, wind profiles for three locations A (28.0 N, 76.0 E), B (30.5 N, 79.1 E) and C (28.0 N, 82.0 E) had been plotted. Region A was representative of flow at the southwestern region facing Arabian Sea, while C characterized the easterly flow from the Bay of Bengal. B signified the vertical developments at the centre of the event. The vertical wind profile at the inflow region corresponding to C showed a strong easterly jet stretching from

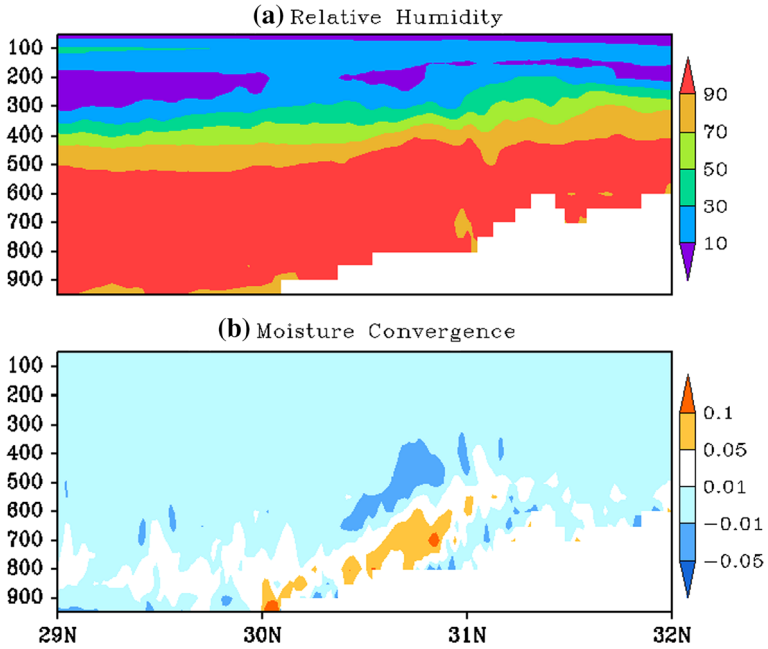


Fig. 8 Vertical distribution of **a** relative humidity (%) and **b** moisture convergence (kg/kg/s) along the latitude. These values represented the average behaviour of longitude 78°E–80°E

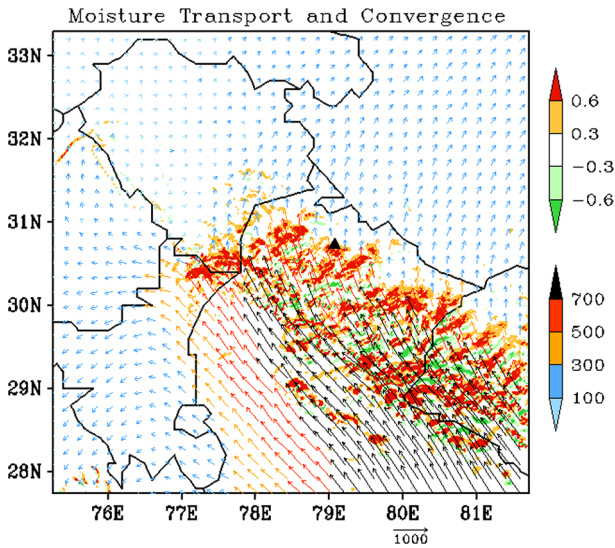


Fig. 9 Spatial distribution of vertically integrated moisture transport (in vector; kg/m/s) and moisture convergence (*shaded*), where dense vectors signified ample supply of moisture. *Triangle* showed the location of Kedarnath region

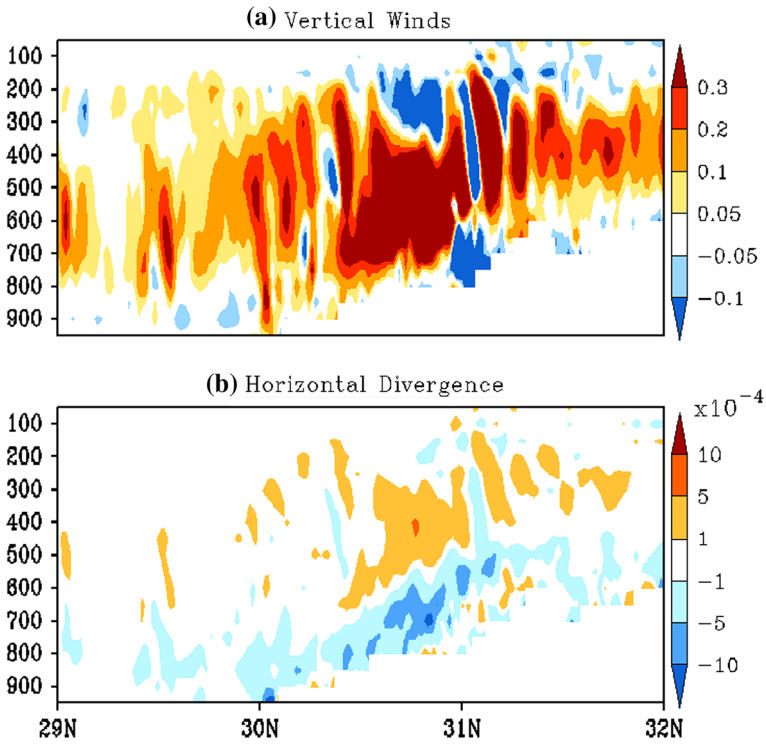


Fig. 10 Vertical distribution of **a** vertical winds (m/s) and **b** horizontal divergence (s^{-1}) along the latitude. These values represented the average behaviour of longitude 78°E–80°E

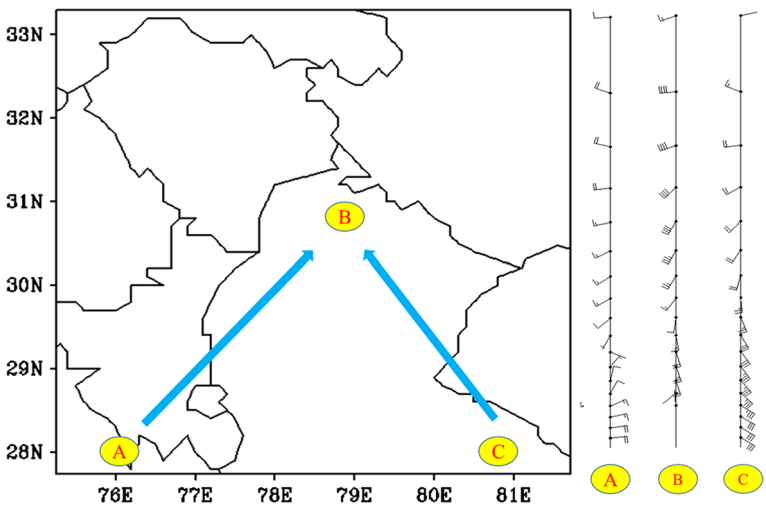


Fig. 11 Wind profiles for three locations A (28.0N, 76.0E), B (30.5N, 79.1E) and C (28.0N, 82.0E). Location B showed the Kedarnath region

900 hPa to 500 hPa and having its maximum near the surface, consistent with the presence of a low-level jet (LLJ). This wind maximum was also evident in the wind field and is shown in Fig. 1, wherein significant easterly flow moved parallel to the Himalayan ranges from 13 June 2013. The build-up of high winds till mid-troposphere was observed due to forced orographic lifting. Earlier studies (Rasmussen and Houze 2012; Kumar et al. 2014a) showed that the low-level moisture flowing upslope into the storm system was of particular importance for many flash flooding events. The most interesting plot was for the region B, which was roughly the convergence point of both the flows and junction of maximum disaster. The veering of wind direction at the upper levels towards eastward direction resulted in near cancellation of advection and storm propagation culminating into a quasi-stationary system. The individual convective updrafts, apparent as strong vertical winds, moved with a speed and direction roughly comparable to the mean flow of the tropospheric layer containing the updraft, which when flowing in a direction opposite to the storm propagation made the system nearly stationary (Doswell et al. 1996). In this particular case, steep terrain-induced updrafts combined with strong large-scale flow and a slow moving system allowed high precipitation rates to persist for a relatively long duration.

6 Conclusion

A simulation study has been performed using WRF model at high resolution for severe rainfall event over Uttarakhand region of India during 16–17 June 2013 which devastated the temple town of Kedarnath. Model predicted rainfall is compared with satellite-derived merged rainfall products. Results show that the WRF model is able to predict the intensity of the Uttarakhand heavy rainfall episode. It is observed that the spatial distribution of heavy rainfall is well captured by the WRF model when verified with satellite-retrieved rainfall products. A comprehensive diagnostic assessment and comparisons of the moisture fields were conducted, wherein we focused on the precipitation and its relationship with moisture transport its divergence/convergence in the atmosphere, and the dependency of vertical development with wind flows in an orographic topography. Vertically integrated moisture transport analysis indicates the convergence of moisture flow in the region triggering and sustaining the intense rainfall episode. The vertical distribution of relative humidity and horizontal divergence also show favourable atmospheric conditions precessing the storm. Moreover, VDEL model initialized from the WRF model showed that the orographic component of rain rate is quite high over this region and suggests that the topography, in particular with its orientation to the low-level wind fields, and the moisture availability had a major role on extreme precipitation event. It is demonstrated in this study that resolving the complex topography at finer scales in a numerical model has the capability to provide higher prediction skill.

Acknowledgments The authors would like to thank Mr. A. S. Kiran Kumar, Chairman, ISRO for constant encouragement and guidance. Authors are also thankful to National Center for Atmospheric Research (NCAR) for WRF model. The global analysed and forecast data provided by National Centers for Environmental Prediction (NCEP) are acknowledged with sincere thanks.

References

- Anabor V, Stensrud DJ, de Moraes OL (2009) Simulation of a serial upstream-propagating mesoscale convective system event over southeastern South America using composite initial conditions. *Mon Weather Rev* 137(7):2144–2163

- Barros AP, Joshi M, Putkonen J, Burbank DW (2000) A study of the 1999 monsoon rainfall in a mountainous region in central Nepal using TRMM products and rain gauge observations. *Geophys Res Lett* 27(22):3683–3686
- Barros AP, Kim G, Williams E, Nesbitt SW (2004) Probing orographic controls in the Himalayas during the monsoon using satellite imagery. *Nat Hazard Earth Syst Sci* 4(1):29–51
- Bauer P, Auligné T, Bell W, Geer A, Guidard V, Heilliette S, Kazumori M, Kim MJ, Liu EHC, McNally AP, Macpherson B, Okamoto K, Renshaw R, Riishøjgaard LP (2011) Satellite cloud and precipitation assimilation at operational NWP centres. *Q J R Meteorol Soc* 137:1934–1951
- Benedetti A, Lopez P, Bauer P, Moreau E (2005) Experimental use of TRMM precipitation radar observations in 1D+4D-Var assimilation. *Q J R Meteorol Soc* 131:2473–2495
- Bohra AK, Basu S, Rajagopal EN, Iyengar GR, Gupta MD, Ashrit R, Athiyaman B (2006) Heavy rainfall episode over Mumbai on 26 July 2005: assessment of NWP guidance. *Curr Sci* 90:1188–1194
- Buzzi A, Foschini L (2000) Mesoscale meteorological features associated with heavy precipitation in southern Alpine region. *Meteorol Atmos Phys* 72:131–146
- Chang HI, Kumar A, Niyogi D, Mohanty UC, Chen F, Dudhia J (2009) The role of land surface processes on the mesoscale simulation of the July 26, 2005 heavy rain event over Mumbai. *India Glob Planet Change* 67:87–103. doi:10.1016/j.gloplacha.2008.12.005
- Das S, Ashrit R, Moncrieff MW (2006) Simulation of a Himalayan cloudburst event. *J Earth Syst Sci* 115:299–313
- Dobhal DP, Gupta AK, Mehta M, Khandelwal DD (2013) Kedarnath disaster: facts and plausible causes. *Curr Sci* 105:171–174
- Doswell CA III, Brooks HE, Maddox RA (1996) Flash flood forecasting: an ingredients-based methodology. *Weather Forecast* 11:560–581
- Dube A, Ashrit R, Ashish A, Sharma K, Iyengar GR, Rajagopal EN, Basu S (2013) Performance of NCMRWF forecast models in predicting the Uttarakhand heavy rainfall event during 17–18 June 2013, NMRF/RR/08/2013
- Dudhia J (1989) Numerical study of convection observed during the winter monsoon experiment using a mesoscale two-dimensional model. *J Atmos Sci* 46:3077–3107
- Francis PA, Gadgil S (2006) Intense rainfall events over the west coast of India. *Meteorol Atmos Phys* 94:27–45
- Goswami BN, Venugopal VD, Sengupta D, Madhusudan MS, Xavier PK (2006) Increasing trend of extreme rain events over India in a warming environment. *Science* 314:1442–1445
- Guhathakurta P, Rajeevan M (2008) Trends in the rainfall pattern over India. *Int J Climatol* 28:1453–1469. doi:10.1002/joc.1640
- Guhathakurta P, Sreejith OP, Menon PA (2011) Impact of climate change on extreme rainfall events and flood risk in India. *J Earth Syst Sci* 120:359–373
- Hong SY, Dudhia J (2003) Testing of a new non-local boundary layer vertical diffusion scheme in numerical weather prediction applications. 20th conference on weather analysis and forecasting/16th conference on numerical weather prediction, Seattle, WA
- Hong SY, Lim JOJ (2006) The WRF single-moment 6-class microphysics scheme (WSM6). *Asia-Pac J Atmos Sci* 42(2):129–151
- Hong SY, Pan HL (1996) Nonlocal boundary layer vertical diffusion in a medium range forecast model. *Mon Weather Rev* 124:2322–2339
- Howarth David A (1983) Seasonal variations in the vertically integrated water vapor transport fields over the southern Hemisphere. *Mon Weather Rev* 111:1259–1272
- Hu XM, Nielsen-Gammon JW, Zhang F (2010) Evaluation of three planetary boundary layer schemes in the WRF model. *J Appl Meteorol Climatol* 49(9):1831–1844
- IMD (2013) A preliminary report on heavy rainfall over Uttarakhand during 16–18 June 2013. India Meteorological Department, Ministry of Earth Sciences; July 2013. http://imd.gov.in/doc/uttrakhand_report_04_09_2013.pdf
- Kain JS, Fritsch JM (1990) A one-dimensional entraining/detraining plume model and its application in convective parameterization. *J Atmos Sci* 47:2784–2802
- Kain JS, Fritsch JM (1993) Convective parameterization for mesoscale models: The Kain–Fritsch scheme. In: The representation of cumulus convection in numerical models, American Meteorological Society, pp. 165–170
- Khaladkar RM, Mahajan PN, Kulkarni JR (2009) Alarming rise in the number and intensity of extreme point rainfall events over the Indian region under climate change scenario. IITM research report No. RR-123, ISSN 0252-1075
- Kishtawal CM, Niyogi D, Tewari M, Roger A, Sr Pielke, Marshall Shepherd J (2010) Urbanization signature in the observed heavy rainfall climatology over India. *Int J Climatol* 30:1908–1916

- Kumar A, Dudhia J, Rotunno R, Niyogi D, Mohanty UC (2008) Analysis of the 26 July 2005 heavy rain event over Mumbai, India using the weather research and forecasting (WRF) model. *Q J R Meteorol Soc* 134:1897–1910
- Kumar A, Houze RA Jr, Rasmussen KL, Peters-Lidard C (2014a) Simulation of a flash flooding storm at the steep edge of the Himalayas. *J Hydrometeorol* 15(1):212–228
- Kumar P, Kishtawal CM, Pal PK (2014b) Impact of direct rainfall assimilation on weather research and forecasting model forecast over tropical region. *J Geophys Res Atmos* 119:2017–2031
- Lopez P (2011) Direct 4D-Var assimilation of NCEP stage IV radar and gauge precipitation data at ECMWF. *Mon Weather Rev* 139:2098–2116
- Ludlam FH (1963) Severe local storms: a review. In: Atlas D (ed) *Severe local storms*, AMS monogr, 27th edn. American Meteorological Society, Boston, pp 1–30
- Mlawer EJ, Taubman SJ, Brown PD, Iacono MJ, Clough SA (1997) Radiative transfer for inhomogeneous atmosphere: RRTM, a validated correlated-k model for the longwave. *J Geophys Res* 102:16663–16682
- Rajeevan M, Bhate J, Jaswal AK (2008) Analysis of variability and trends of extreme rainfall events over India using 104 years of gridded daily rainfall data. *Geophys Res Lett* 35:L18707. doi:[10.1029/2008GL035143](https://doi.org/10.1029/2008GL035143)
- Rasmussen KL, Houze RA Jr (2012) A flash-flooding storm at the steep edge of high terrain disaster in the Himalayas. *Bull Am Meteorol Soc* 93:1713–1724
- Reale O, Feudale L, Turato B (2001) Evaporative moisture sources during a sequence of floods in the mediterranean region. *Geophys Res Lett* 28:2085–2088
- SenRoy S, Balling RC (2004) Trends in extreme daily precipitation indices in India. *Int J Climatol* 24:457–466
- Sinclair MR (1994) A diagnostic model for estimating orographic precipitation. *J Appl Meteorol* 33:1163–1175
- SinhaRay KC, De US (2003) Climate change in India as evidenced from instrumental records. *WMO Bull* 52:53–59
- Skamarock WC, Klemp JB, Dudhia J, Gill DO, Barker DM, Duda MG, Huang XY, Wang W, Powers JG (2008) A description of the advanced research WRF Version 3. NCAR/TN-475 STR; NCAR technical note, Mesoscale and Microscale Meteorology Division, National Center of Atmospheric Research, pp. 113
- Srinivasan J (2013) Predicting and managing extreme rainfall. *Curr Sci* 105:7–8
- Thompson CS, Sinclair MR, Gray WR (1997) Estimating long-term annual precipitation in a mountainous region from a diagnostic model. *Int J Climatol* 17(9):997–1007
- Wang C, Gao S, Liang L, Deng D, Gong H (2014) Multi-scale characteristics of moisture transport during a rainstorm process in North China. *Atmos Res* 145:189–204